Available online at www.sciencedirect.com
ScienceDirect
Trans. Nonferrous Met. Soc. China 24(2014) 2122−2129
Transactions of Nonferrous Metals Society of China
www.tnmsc.cn

Non-isothermal retrogression kinetics for grain boundary precipitate of 7A55 aluminum alloy

Di FENG[1,2], Xin-ming ZHANG[1,2], Sheng-dan LIU[1,2], Ze-zheng WU[1,2], Ting WANG[1,2]

1. School of Materials Science and Engineering, Central South University, Changsha 410083, China;
2. Key Laboratory of Nonferrous Metal Materials Science and Engineering of Ministry of Education, Central South University, Changsha 410083, China

Received 17 October 2013; accepted 16 April 2014

Abstract: The retrogression kinetics for grain boundary precipitate (GBP) of 7A55 aluminum alloy was investigated by transmission electron microscopy (TEM) observation. The results reveal that the coarsening behavior of GBP obeys "LSW" theory, namely, the cube of GBP average size has a linear dependence relation to retrogression time, and the coarsening rate accelerates at the elevated retrogression temperature. The GBP coarsening activation energy Q_d of (115.2±1.3) kJ/mol is obtained subsequently. Taking the retrogression treatment schedule of 190 °C, 45 min derived from AA7055 thin plate as reference, the non-isothermal retrogression model for GBP coarsening behavior is established based on "LSW" theory and "iso-kinetics" solution, which includes an Arrhenius form equation. After that, the average size of GBP $r(t)$ is predicted successfully at any non-isothermal process $T(t)$ when the initial size of GBP r_0 is given. Finally, the universal characterization method for the microstructure homogeneity along the thickness direction of 7A55 aluminum alloy thick plate is also set up.

Key words: non-isothermality; retrogression kinetic; 7A55 aluminum alloy; grain boundary precipitate

1 Introduction

Temperature gradients exist in 7xxx series aluminum alloy thick plates during heat treatments because of the heat conduction problem, so the heat treatment of 7xxx series aluminum alloy plate is a non-isothermal process [1−3]. In non-isothermal reactions, the thermodynamic parameters of aluminum alloy, such as the diffusion coefficient (especially in heating or cooling stage), nucleation driving force and nucleation barrier, are influenced by temperature variation. As one of the typical non-isothermal treatment technologies, the retrogression and re-aging treatment (RRA), in which the precipitates experience re-dissolution, nucleation, growth or coarsening reactions simultaneously, has a more rigorous requirement to the retrogression temperature and time. Consequently, the non-isothermal stage during retrogression results in non-homogeneity of microstructures along the thickness direction in 7xxx series aluminum plates [4,5]. The establishment of an optimized retrogression and re-aging technological procedure needs a systematic study of microstructure evolution during non-isothermal reactions. However, a large number of investigations are all focused on isothermal treatment. SHERCLIFF and ASHBY [6,7] established a model to predict the age hardening behaviour of aluminum alloys. For Al−Zn−Mg−Cu alloys, GUYOT and COTTIGNIES [8] and STARINK and WANG [9] investigated the relationships between precipitate kinetics and electrical conductivity or yield strength. Only NICOLAS and DESCHAMPS [10] and HUTCHINSON et al [11] investigated the precipitation behaviours of Al−Zn−Mg−Cu alloy under non-isothermal treatment. However, for retrogression, as mentioned above, it is difficult to research the microstructure evolution of matrix precipitates by physical experiments due to the diversifications of precipitate's kinds and reaction behaviors [12−14]. Fortunately, the grain boundary owns homogeneous types of precipitate of η phase, and its retrogression behavior is relatively simple [15−18]. So, the GBP retrogression behavior of 7A55 aluminum alloy is studied under different retrogression conditions by

Foundation item: Project (2012CB619505) supported by the National Basic Research Program of China
Corresponding author: Xin-ming ZHANG; Tel: +86-731-88830265; E-mail: xmzhang_cn@aliyun.com
DOI: 10.1016/S1003-6326(14)63322-7

isothermal treatment firstly, and then the non-isothermal retrogression model for GBP coarsening behavior is established according to the "iso-kinetics" approach. The purpose of this work is the calculation of the average size of GBP and setting up a universal characterization method for the microstructure homogeneity along the thickness direction of 7A55 aluminum alloy plate.

2 Modeling approach

2.1 Iso-kinetic assumption

A reaction is regarded as iso-kinetic if the increments of transformation in infinitesimal isothermal time steps are additive. GRONG et al [4,19,20] defined this mathematically by stating that a reaction is iso-kinetic if the evolution equation for some state variable S may be written in the form:

$$\frac{\mathrm{d}S}{\mathrm{d}t}=\frac{G(S)}{H(T)} \tag{1}$$

where $G(S)$ and $H(T)$ are arbitrary functions of state variable S and temperature T, respectively. Equation (1) is a separable differential equation, and the integral representation is shown as follows:

$$\int_0^S \frac{\mathrm{d}S}{G(S)}=\int_0^t \frac{\mathrm{d}t}{H(T)} \tag{2}$$

The integral on the right hand side is termed as the "kinetic strength" [6−8]. The function $H(T)$ will evolve to a time constant which includes the temperature dependence if S is a dimensionless parameter. In that case, the "kinetic strength" reduces to Scheil integral [4]. Under isothermal conditions, the total time to reach $S=S_\mathrm{c}$ is simply obtained by adding the fractions of temperature-weighted time until the kinetic strength integral is equal to unity [4].

The relationship between Scheil integral and diffusional transformation can be substantiated through Fick' second law:

$$\begin{cases}\dfrac{\partial C}{\partial \tau}=[\nabla^2 C]\\ \tau=\displaystyle\int_0^t D(t)\mathrm{d}t\end{cases} \tag{3}$$

By introducing the scaled parameter $I=\tau/(D_0t_\mathrm{r})$, where D_0 and t_r are the per-exponential term in the expression for the diffusion coefficient and an arbitrarily chosen reference time, Eq. (3) can be rewritten as

$$I=\int_0^t \frac{\mathrm{d}t}{t_0^*} \tag{4}$$

where $t_0^*=t_\mathrm{r}\exp[Q_\mathrm{d}/(RT)]$ is the temperature-dependent time constant.

2.2 Iso-kinetic solution of LSW theory

LIFSHITZ and SLYOZOV [21] considered that the particle coarsening kinetics is controlled by volume diffusion through the matrix. Provided that no solute is lost to the surrounding matrix during the process ($\mathrm{d}f/\mathrm{d}t=0$), the time dependence of the mean particle radius r can be written as

$$r^3(t)-r_0^3=\frac{c_1 t}{T}\exp\left(-\frac{Q_\mathrm{d}}{RT}\right) \tag{5}$$

$$K=\frac{c_1}{T}\exp\left(-\frac{Q_\mathrm{d}}{RT}\right)=\frac{8v\gamma C_\mathrm{eq}D}{9R}=\frac{8v\gamma C_\mathrm{eq}D_0}{9RT}\exp\left(-\frac{Q_\mathrm{d}}{RT}\right) \tag{6}$$

where v is the atom volume of precipitate; γ is the interfacial energy between precipitate and matrix; C_eq is the precipitate/matrix interfacial concentration; D is the diffusion coefficient of solute atom; c_1 is a kinetic constant; r_0 and Q_d are initial radius and the activation energy for precipitate coarsening, respectively; K is an artificial variable. The coarsening kinetics model expressed by Eq. (5) is called "LSW" theory. Equation (5) can be written in a dimensionless form by introducing:

$$S=\frac{r^3-r_0^3}{r_0^3}=\frac{c_1 t}{r_0^3 T}\exp\left(-\frac{Q_\mathrm{d}}{RT}\right) \tag{7}$$

Let t_r denote the time taken to reach a certain value $S=S_\mathrm{r}$ at a chosen reference temperature $T=T_\mathrm{r}$, Eq. (7) can be represented as follows:

$$S=S_\mathrm{c}=\frac{c_1 t_\mathrm{r}}{r_0^3 T_\mathrm{r}}\exp\left(-\frac{Q_\mathrm{d}}{RT_\mathrm{r}}\right) \tag{8}$$

Dividing Eq. (7) by Eq. (8):

$$\frac{S}{S_\mathrm{c}}=\frac{T_\mathrm{r}t}{t_\mathrm{r}T}\exp\left[\frac{Q_\mathrm{d}}{R}\left(\frac{1}{T_\mathrm{r}}-\frac{1}{T}\right)\right] \tag{9}$$

then, Eq. (9) evolves to Eq. (10) by introducing the time constant t^*:

$$\begin{cases}t^*=t_\mathrm{r}\dfrac{T}{T_\mathrm{r}}\exp\left[\dfrac{Q_\mathrm{d}}{R}\left(\dfrac{1}{T}-\dfrac{1}{T_\mathrm{r}}\right)\right]\\ S=S_\mathrm{c}\dfrac{t}{t^*}\end{cases} \tag{10}$$

In order to obtain the desired iso-kinetic solution, Eq. (10) needs to be rewritten in a differential form and integral the left and the right hand sides independently:

$$\begin{cases}\dfrac{\mathrm{d}S}{\mathrm{d}t}=\dfrac{S_\mathrm{c}}{t^*}\\ S=S_\mathrm{c}\displaystyle\int_0^t \frac{\mathrm{d}t}{t^*}\end{cases} \tag{11}$$

If the mean size of grain boundary precipitate is treated as state variable, the non-isothermal can be established when the thermal history and coarsening activation energy are obtained.

As mentioned in the introduction above, the RRA treatment in 7A55 aluminum alloy thick plate is a non-isothermal process. Therefore, the innovation of “non-isothermal retrogression kinetics model” in this work is the integrated utilization of “iso-kinetic assumption” and “LSW” theory under isothermal condition to the research of non-isothermal RRA treatment. After the non-isothermal model establishment, it is possible to forecast through thickness microstructural homogeneity.

3 Experimental

The material used in this work is a commercial aluminum alloy 7A55 in the form of 30 mm thick plate. The composition of the alloy is: Al−7.68Zn−2.12Mg−1.98Cu−0.055Fe−0.034Si−0.12Zr (mass fraction, %). Two types of samples including flake and block are used in the experiments. The flake samples (20 mm×15 mm×2 mm) are cut from LTD-RD plane for project A. The samples are all solution treated under (470 °C, 1 h)+(480 °C, 1 h) condition, quenched into water, and then aged in three steps as described in Table 1. The results of project A are used for the statistics of grain boundary precipitates dimensions, the calculation of coarsening activation energy and the establishment of the non-isothermal retrogression model for GBP coarsening behavior, while the results of project B are used to validate the model. Retrogression and re-aging treatments are marked as R-*x* min and RRA-*x* min, where *x* represents the retrogression time.

Table 1 Description of retrogression and re-aging treatments

Experimental project	Pre-aging	Retrogression
A	65 °C, 24 h	170 °C, *x* min
		190 °C, *x* min
		200 °C, *x* min
B	65 °C, 24 h 120 °C, 24 h	190 °C, 45 min

Note: Retrogression heating rate: 5 °C/min; Re-aging: 120 °C, 24 h

The thermal history of retrogression in 30 mm plates along the thickness direction is measured by thermoelectric couple, and registered by computer. The development of microstructure during retrogression and re-aging is studied by means of transmission electron microscopy (TEM) observation. Specimens for TEM observations are electropolished in the solution of 20% HNO_3 in methanol at ~−25 °C and 15−20 V. The thin foils are examined with a TecnaiG^2 20 TEM operated at 200 kV.

4 Results and discussion

4.1 Establishment of model

The results from TEM observations of the retrogression microstructures are summarized in Fig. 1. The matrix and grain boundary precipitate (GPB) experience Ostwald ripening both with the increase of time and the rise of retrogression temperature, and the coarsening rate accelerates at the elevated retrogression temperature. The coarsening behavior of GBP is evident due to the preferential precipitated tendency at grain boundary. The precipitates free-zones are also broadened with the temperature and time increasing.

GBP has limited coarsening extent when retrogressed at 170 °C. After 90 min retrogression treatment, the average size is only 32.8 nm and most parts of GBP maintain continuous contribution as a chain. The precipitates free-zones are narrow, and the width is about 35 nm. However, with the retrogression temperature increasing, coarsening extent is enhanced greatly. The average sizes of GBP are 56.2 and 69.8 nm, respectively after being retrogressed for 90 min at 190 °C and 200 °C, meanwhile, the precipitates free-zones are broadened to 60−70 nm.

The relationships between the average size of GBP and retrogression time at different temperatures are fitted in Fig. 2(a). Results show that the coarsening behavior of GBP of 7A55 aluminum alloy obeys LSW theory (Eq. (5)), namely, the cubic of GBP average size has a linear dependence relation to retrogression time, and the coarsening rate accelerates at the elevated retrogression temperature.

Equation (6) can be rewritten as

$$\ln(KT) = \ln c_1 - \frac{Q_\mathrm{d}}{RT} \tag{12}$$

For each retrogression time, K is determined by the slope of R^3 vs isothermal time t (Fig. 2(a)), then the activation energy Q_d can be obtained using plot of $\ln(KT)$ vs $1/T$ (Fig. 2(b)). By this mean, the activation energy of GBP for 7A55 aluminum alloy during retrogression estimated from Eq. (12) is (115.2±1.3) kJ/mol, which is a little lower than that of the matrix precipitate (117.1−120 kJ/mol) [22]. The grain boundary has a higher interfacial energy level, which reduces the energy barrier of solute atom diffusion.

Set reference temperature and time as 190 °C and 45 min, respectively, then the temperature−dependent time constant t^* can be expressed as

$$t^* = 5.83T(t)\exp\left[1.4\times10^4\left(\frac{1}{T(t)} - \frac{1}{463}\right)\right] \tag{13}$$

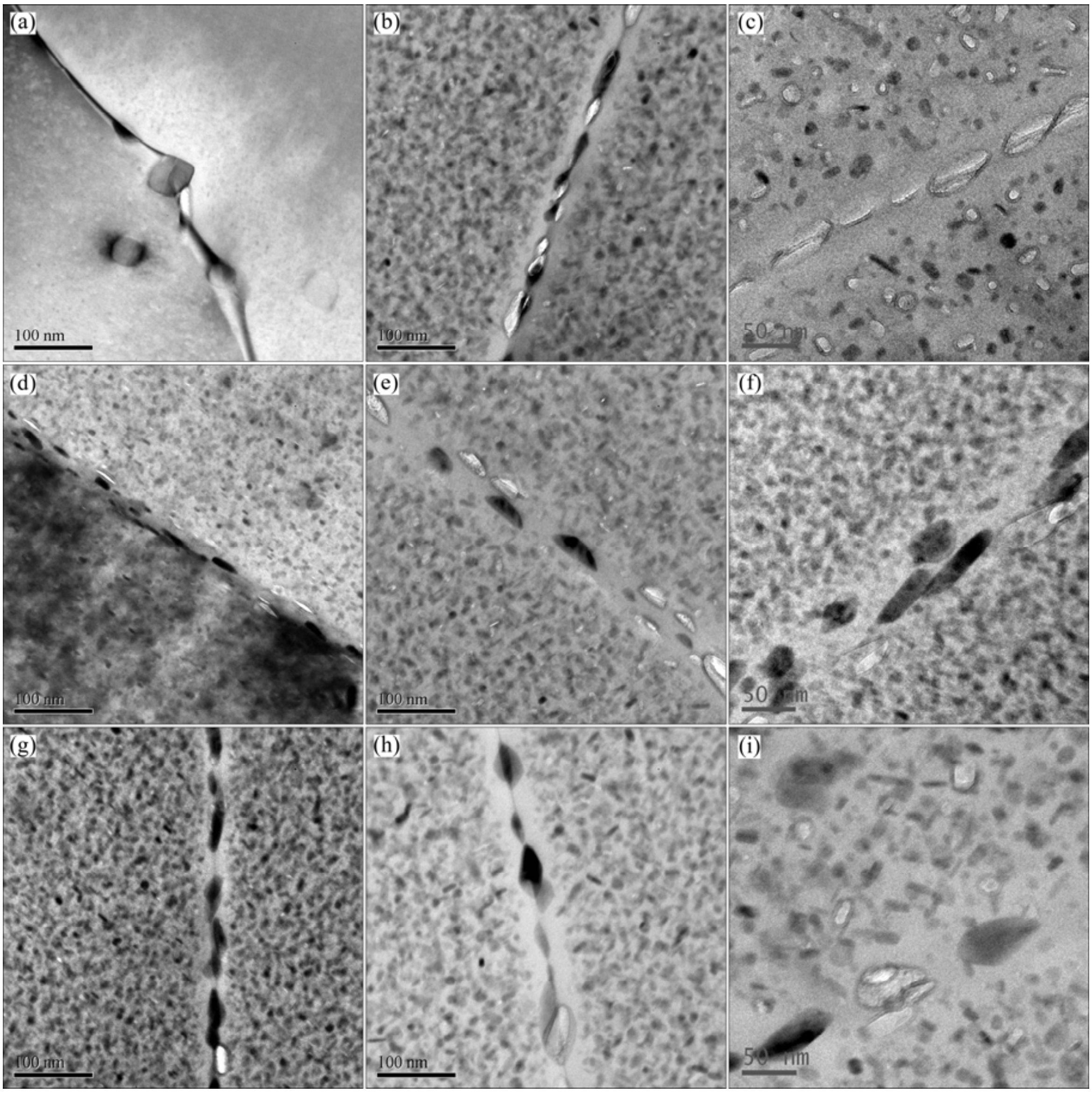

Fig. 1 Microstructures of flake samples under different retrogression treated under isothermal conditions: (a) 170 °C/10 min; (b) 170 °C, 45 min; (c) 170 °C, 90 min; (d) 190 °C, 10 min; (e) 190 °C, 45 min; (f) 190 °C, 90 min; (g) 200 °C, 10 min; (h) 200 °C, 45 min; (i) 200 °C, 90 min

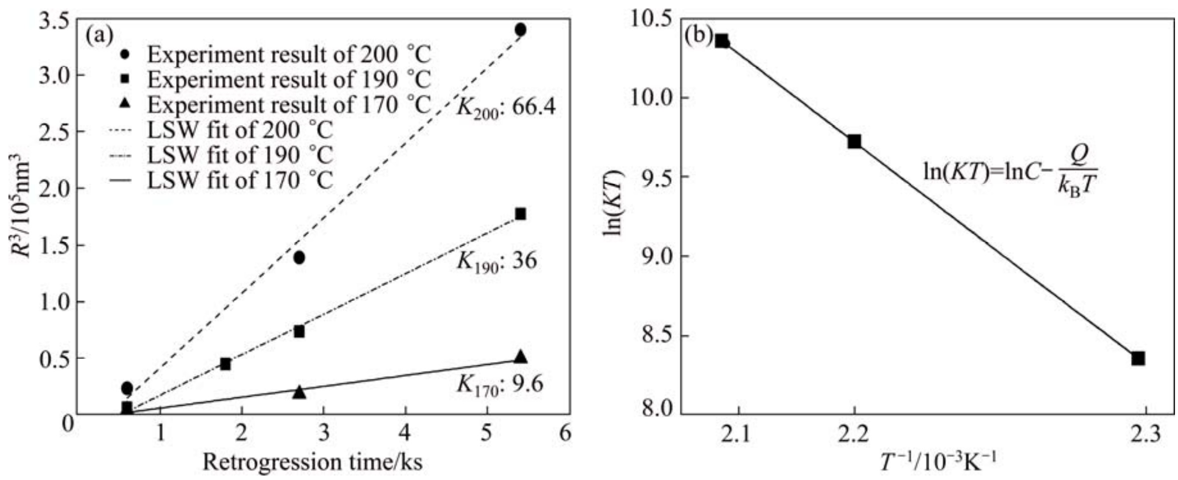

Fig. 2 Relationship of R^3 vs retrogression time (a) and ln(KT) vs (1/T) (b)

Based on Eq. (12), the non-isothermal retrogression model for GBP coarsening behavior is established as

$$\begin{cases} S = S_c \int_0^t \dfrac{\exp[1.4\times10^4(\dfrac{1}{463}-\dfrac{1}{T(t)})]}{5.83T(t)}\mathrm{d}t \\ r^3(t) = r_0^3(t)(1+S) \end{cases} \tag{14}$$

4.2 Validation of model

Correlations of retrogression temperature with the time under different pre-ageing temperature conditions are shown in Fig. 3. There are temperature differences between the surface, sub-surface and central layer during heating processes. The surface layer has the highest temperature raising rate.

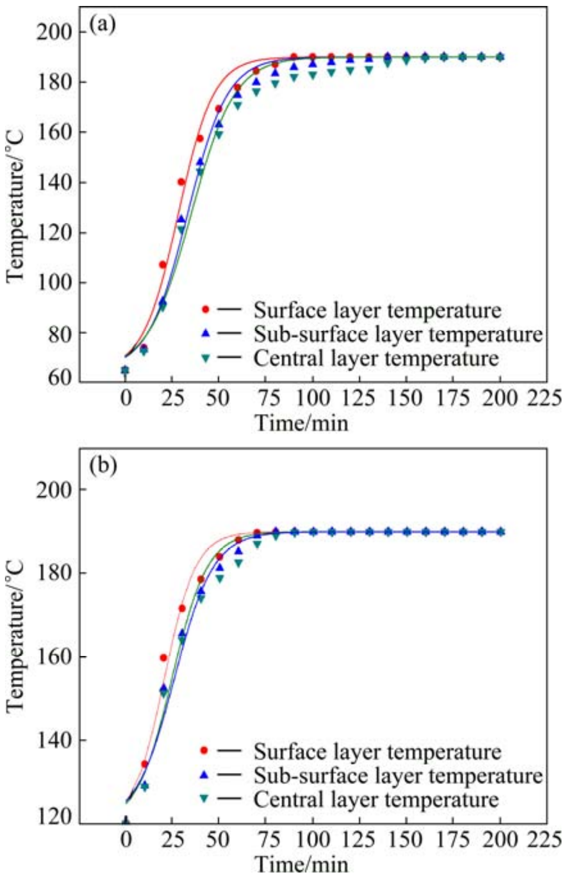

Fig. 3 Retrogression temperature−time curves of 30 mm plates of 7A55 aluminum along thickness direction: (a) (65 °C, 24 h)+ 5 °C/min+190 °C; (b) (120 °C, 24 h)+5 °C/min+190 °C

It could be noted from Fig. 3 that the temperature rising time is shorter under higher pre-aging temperature condition (Fig. 3(b)), and the stable temperature after heating is also a little higher than that of lower pre-aging temperature. However, the whole plate does not achieve the presuppose retrogression temperature after heating no matter what the pre-aging temperature is. In other words, the so-called “heat preservation stage” is still a non-isothermal process. In this stage, the temperature raising rate is inversely higher because the low pre-aging temperature leads to higher temperature gradient, which reduces the impact from pre-aging temperature to retrogression temperature.

The thermal histories of different layers in Eq. (14) are substituted by the outcomes of model fitting in a sigmoidal manner (Fig. 3). After that, the average size evolution of grain boundary precipitate in different layers with retrogression time variation is obtained by calculation in Matlab using a subroutine.

The GBP size evolution with retrogression time for different layers of 7A55 aluminum plates is shown in Fig. 4. It is noted that the growth rates of GBP are slow (Figs. 4(a) and (b)) in both two pre-aging treatmented samples due to the lack of coarsening driving force under low temperature in the heating stages, and the coarsening start time is a little earlier in peak pre-aging treatment one. After heating, the atmosphere temperature in furnace is as high as the presupposed retrogression temperature, so the temperature raising rate of 7A55 aluminum alloy plate accelerates due to the high temperature gradients. At this moment, the average size of GBP coarsens fast with retrogression time, and the

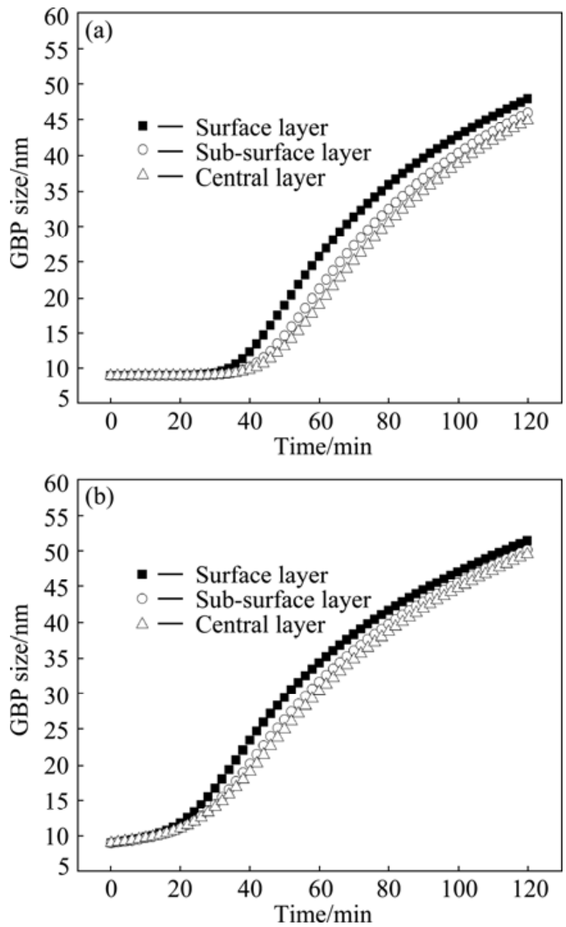

Fig. 4 Correlations between GBP size and retrogression time for different layers of 7A55 aluminum plates: (a) (65 °C, 24 h) + 5 °C/min + (190 °C, x min); (b) (120 °C, 24 h) + 5 °C/min + (190 °C, x min)

coarsening rate has a marked increase. However, the temperature raising rate decreases as retrogression time extends further, resulting in a reduction of coarsening rate.

The TEM observations of precipitates in surface and central layers under different aging treatments are shown in Fig. 5. It can be observed that the GBP are broken completely in both of the two heat treatments and precipitate-free zones of 40−50 nm width appear. The statistics of average size of GBP are carried out in a multiple view, and the results are compared with the calculation ones using the non-isothermal retrogression model in Table 2. The values of average size of GBP predicted from model are found to be fairly close to the experimental values. Parts of the results are greater than those of experiments, which are likely caused by the deviations of temperature measurement or formula fitting of temperature−time.

4.3 Universal characterization method for microstructure homogeneity

Based on Eq. (7) and Eq. (11), an universal characterization method for the microstructure homogeneity along the thickness direction of 7A55 aluminum alloy plate can be obtained:

$$H_{\text{Scheil}}=\frac{R_i}{R_j}\approx\left(\frac{1+\text{Scheil}_i}{1+\text{Scheil}_j}\right)^{\frac{1}{3}}$$
$$=\begin{cases}=1, \text{ homogeneity}\\ \neq 1, \text{ non}-\text{homogeneity}\end{cases} \tag{15}$$

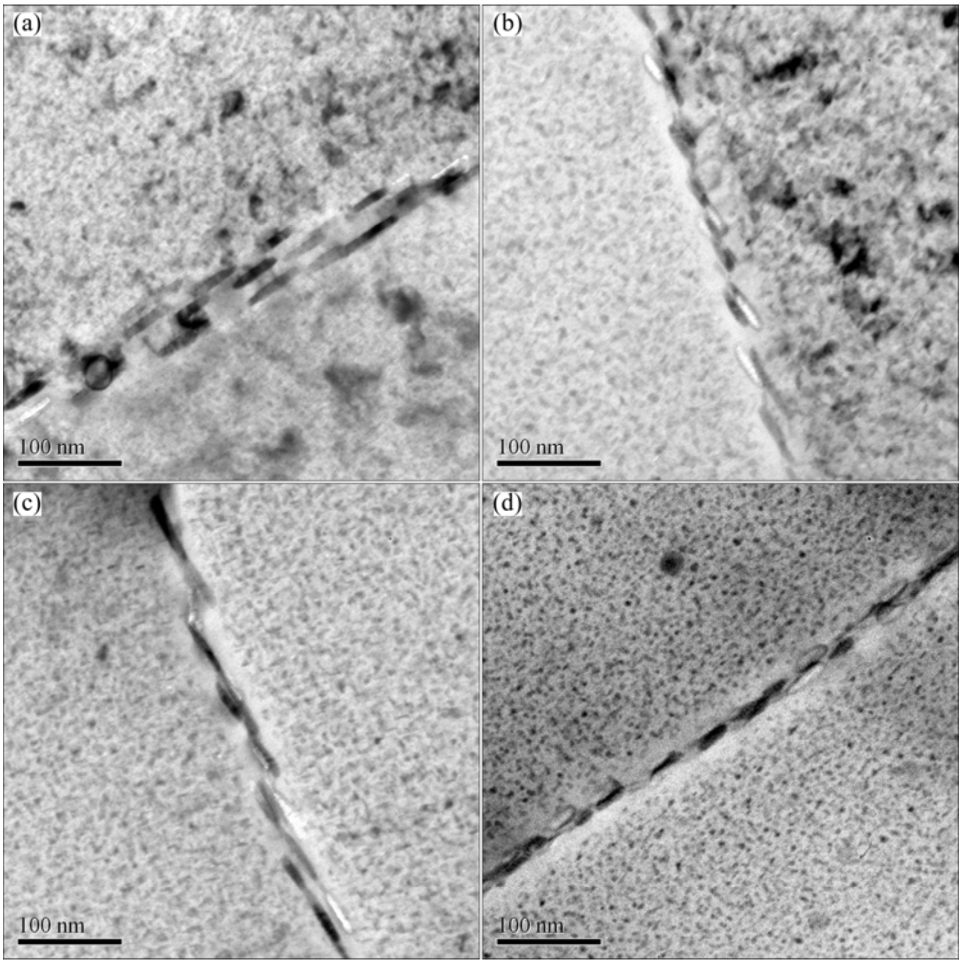

Fig. 5 Microstructures of surface layer (a, b) and central layer (c, d) for 30 mm thick plates: (a, c) (120 °C, 24 h) + 5 °C/min + (190 °C, 45 min); (b, d) (65 °C, 24 h) + 5 °C/min + (190 °C, 45 min)

Table 2 Comparison of average GBP sizes used for validation non-isothermal model

RRA treatment	Surface layer/nm		Central layer/nm	
	Experiment	Calculated	Experiment	Calculated
(120 °C, 24 h) + 5 °C/min + (190 °C, 45 min) + (120 °C, 24 h)	33.6±2.9	34.4	29.3±2.4	30.3
(65 °C, 24 h) + 5 °C/min + (190 °C, 45 min) + (120 °C, 24 h)	31.2±2.7	31.3	26.6±3.3	25.2

where H_{Scheil} represents the through-thickness homogeneity of a plate; R and Scheil are the average size of GBP and the Scheil integral corresponding to the appointed layer (i and j represent the different layers).

The advantage of this method lies in the fact that the microstructure homogeneity along the thickness direction of 7A55 aluminum alloy plate could be predicted conveniently without knowing the initial size of GBP. The representations for the microstructure homogeneity with Scheil integral and size difference between surface and central layer are shown in Fig. 6.

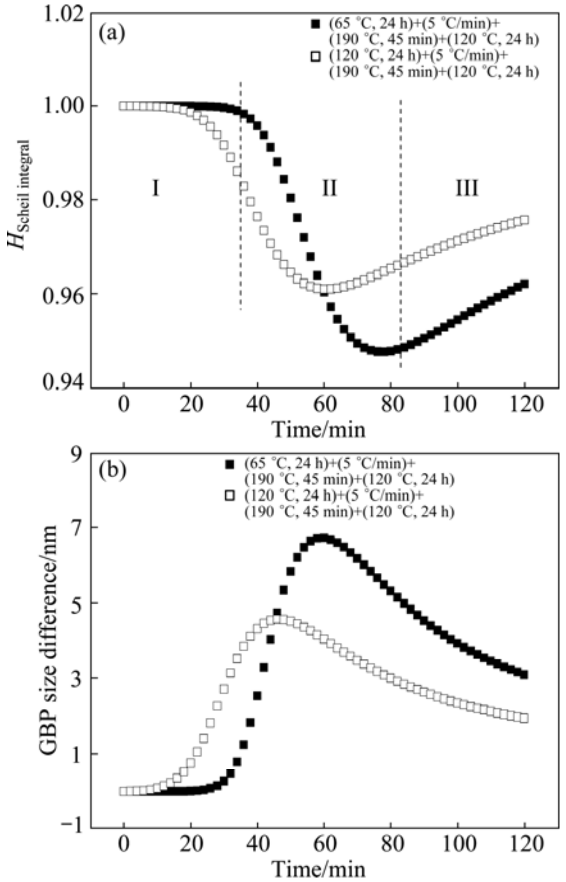

Fig. 6 Representations for microstructure homogeneity along thickness direction of 7A55 aluminum alloy plate: (a) Scheil integral method; (b) Size difference method

Compared to the size difference representation method, Scheil integral depicts the relationship between homogeneity and retrogression time explicitly. It can be summarized that the microstructure homogeneity of 7A55 thick plate decreases with the prolonging of retrogression time before the temperature stabilized stage, and the decreasing rates experience a transformation of slow-quick-slow. However, when the retrogression temperature is reached, an increase of microstructure homogeneity appears. The evolution of homogeneity can be decomposed into a number of stages: 1) Heating. At this stage, the temperature differences between different layers are small (Fig. 3), and the coarsening degree is low due to the lack of coarsening power. Pre-aging microstructure is preserved, thus the Scheil integral has almost no descent. 2) Temperature quick rising. The presupposed retrogression temperature of furnace atmosphere is reached. Temperature difference between the plate and environment is amplified, and the surface layer has the largest temperature raising rate, which brings about a distinct non-homogeneity of GBP coarsening degree of different layers, therefore, Scheil integral drops largely at this moment. 3) Temperature stabilized stage. The temperature of the whole plate tends toward stabilization at the retrogression temperature, as a result, the coarsening rates of different layers turn out to be aligned, so the Scheil integral returns again, which means that the size differences between different layers are narrowed (Fig. 4(b)).

5 Conclusions

1) With the increase of retrogression time and the rise of retrogression temperature, the grain boundary precipitate (GBP) of 7A55 aluminum alloy experiences Ostwald ripening, while the coarsening rate accelerates at the elevated retrogression temperature. The coarsening behavior of GBP obeys LSW theory, and the coarsening activation energy is (115.2±1.3) kJ/mol.

2) The non-isothermal retrogression model for GBP coarsening behavior is established based on the "iso-kinetics" approach.

$$\begin{cases} S = S_c \int_0^t \dfrac{\exp[1.4\times10^4(\dfrac{1}{463}-\dfrac{1}{T(t)})]}{5.83T(t)}\mathrm{d}t \\ r^3(t) = r_0^3(t)(1+S) \end{cases}$$

The average size of GBP is predicted successfully at any transient temperature.

3) The universal characterization method using "Scheil integral" for the microstructure homogeneity along the thickness direction of 7A55 aluminum alloy plate is set up. The microstructure homogeneity of 7A55 aluminum alloy thick plate decreases with the retrogression time extending before the temperature stabilized stage, and the decreasing rate experiences a transformation of slow-quick-slow.

References

[1] CINA B. Reducing the susceptility of alloys, particularly aluminium alloys to stress cracking: U S Patent, 3856584[P]. 1974−02−24.

[2] TALIANKER M, CINA B. Retrogression and reaging and the role of dislocations in the stress corrosion of 7000-type aluminum alloys [J]. Metallurgical and Materials Transactions A, 1989, 20: 2087−2092.

[3] FENG Chun, LIU Zhi-yi, NING Ai-lin, ZENG Su-min. Research and progress in retrogression and reaging treatment of super-high strength aluminum alloy [J]. Materials Review, 2006, 20(4): 98−101.

(in Chinese)
[4] GRONG Ø, SHERCLIFF H R. Microstructural modelling in metals processing [J]. Progressing in Materials Science, 2002, 47: 163−282.
[5] ZHANG Xue. Study on the microstructure evolution of 7050 aluminum alloy during non-isothermal aging process [D]. Harbin: Harbin Institute of Technology, 2012: 11−12. (in Chinese)
[6] SHERCLIFF H R, ASHBY M F. A process model for age hardening of aluminum alloys—I The model [J]. Acta Metallurgica, 1990, 38: 1789−1802.
[7] SHERCLIFF H R, ASHBY M F. A process model for age hardening of aluminum alloys—II Applications of the model [J]. Acta Metallurgica, 1990, 38: 1803−1812.
[8] GUYOT P, COTTIGNIES L. Precipitate kinetics, mechanical strength and electrical conductivity of AlZnMgCu alloys [J]. Acta Materialia, 1996, 44: 4161−4167.
[9] STARINK M J, WANG S C. A model for the yield strength of overaged Al−Zn−Mg−Cu alloys [J]. Acta Materialia, 2003, 51: 5131−5150.
[10] NICOLAS M, DESCHAMPS A. Characterisation and modelling of precipitate evolution in an Al−Zn−Mg alloy during non-isothermal heat treatments [J]. Acta Materialia, 2003, 51: 6077−6094.
[11] HUTCHINSON C R, GOUNE M, REDJAIMIA A. Selecting non-isothermal heat treatment schedules for precipitation hardening systems: An example of coupled process–property optimization [J]. Acta Mater, 2007, 55: 213−223.
[12] ZHANG Yu-hua, YANG Shu-cai, JI Hong-zhi. Microstructure evolution in cooling process of Al−Zn−Mg−Cu alloy and kinetics description [J]. Transactions of Nonferrous Metals Society of China, 2012, 22: 2087−2091.
[13] TANG Jian-guo, CHEN Hui, ZHANG Xin-ming, LIU Sheng-dan, LIU Wen-jun, OUYANG Hui, LI Hong-ping. Influence of quench-induced precipitation on aging behavior of Al−Zn−Mg−Cu alloy [J]. Transactions of Nonferrous Metals Society of China, 2012, 22: 1255−1263.
[14] PENG Guo-sheng, CHEN Kang-hua, CHEN Song-yi, FANG Hua-chan. Influence of dual retrogression and re-aging temper on microstructure, strength and exfoliation corrosion behavior of Al−Zn−Mg−Cu alloy [J]. Transactions of Nonferrous Metals Society of China, 2012, 22: 803−809.
[15] ZHANG Xin-ming, LI Peng-hui, LIU Sheng-dan, ZHU Hang-fei, ZHOU Xin-wei. Effect of retrogression time on intergranular corrosion of 7050 aluminum alloy [J]. The Chinese Journal of Nonferrous Metals, 2008, 18(10): 1795−1804. (in Chinese)
[16] LI Guo-feng, ZHANG Xin-ming, LI Peng-hui. Microstructure evolution rules for aluminum alloy 7050 during retrogression heating up [J]. Rare Metal Materials and Engineering, 2011, 40(7): 1295−1299. (in Chinese)
[17] CHEN Jun-zhou. Precipitate behavior and mechanical properties of AA 7055 aluminum alloy [D]. Harbin: Harbin Institute of Technology, 2008: 6−7. (in Chinese)
[18] OLIVERIAL A F J, de BARROS M C, CARDOSO K R. The effect of RRA on the strength and SCC resistance on AA7050 and AA7150 aluminum alloys [J]. Materials Science and Engineering A, 2004, 379: 321−326.
[19] BJØRNEKLETT1 B I, GRONG Ø, MYHR O R, KLUKEN A O. Additivity and isokinetic behaviour in relation to particle dissolution [J]. Acta Materialia, 1998, 46: 6257−6266.
[20] GRONG Ø, MYHR O R. Additivity and isokinetic behaviour in relation to diffusion controlled growth [J]. Acta Materialia, 2000, 48: 445−452.
[21] LIFSHITZ I M, SLYOZOV V V. The kinetics of precipitate from supersaturated solid solutions [J]. Journal of Physics and Chemistry of Solids, 1961, 19: 35−50.
[22] DU Zhi-wei, ZHOU Tie-tao, LIU Peng-ying, LI Hua-xi, DONG Bbao-zhong, CHEN Chang-qi. Small angle X-ray scattering study of precipitate kinetics in Al−Zn−Mg−Cu alloys [J]. Journal of Materials Science and Technology, 2005, 21: 479−483.

7A55 铝合金晶界析出相的非等温回归动力学

冯 迪[1,2]，张新明[1,2]，刘胜胆[1,2]，吴泽政[1,2]，王 婷[1,2]

1. 中南大学 材料科学与工程学院，长沙 410083；
2. 中南大学 教育部有色金属材料与工程重点实验室，长沙 410083

摘 要：采用 TEM 研究了 7A55 合金回归过程中晶界析出相的动力学行为。研究结果表明：晶界析出相的粗化遵循“LSW”理论，即晶界相平均尺寸的三次方与回归温度呈线性关系，且晶界相的粗化速率随着回归温度的升高而增大。计算得到 7A55 合金晶界析出相的粗化激活能为(115.2±1.3) kJ/mol。将 7A55 铝合金薄板的理论回归制度(190 °C，45 min)作为参考，基于“LSW”理论和“等动力学”处理方法，建立了包含 Arrhenius 方程形式的 7A55 铝合金晶界相非等温回归模型。当初始晶界相尺寸 r_0 已知时，利用该模型可成功预测非等温回归阶段任意时间点的晶界相平均尺寸 $r(t)$。在此基础上，最终建立了一种 7A55 铝合金厚板高向组织均匀性的通用表征方法。

关键词：非等温；回归动力学；7A55 铝合金；晶界相

(Edited by Yun-bin HE)